The Future 5G Network-Based Secondary Load Frequency Control in Shipboard Microgrids

Gheisarnejad, M.; Khooban, M.; Dragicevic, T.

Published in:
IEEE Journal of Emerging and Selected Topics in Power Electronics

DOI (link to publication from Publisher):
10.1109/JESTPE.2019.2898854

Publication date:
2020

Document Version
Accepted author manuscript, peer reviewed version

Journal of Emerging and Selected Topics in Power Electronics

The Future 5G Network Based Secondary Load Frequency Control in Maritime Microgrids

Meysam Gheisarnejad, Mohammad-Hassan Khooban, *Senior, IEEE,* Tomislav Dragicevic, *Senior Member*

***Abstract*—This paper presents the applicability of the future fifth generation (5G) network technology for a marine vessel power system with the sea wave energy (SWE), Photovoltaic (PV) and energy storage systems (ESSs). In this study, a new optimal structured interval type-2 fractional order fuzzy PD/fuzzy PI (IT2FO-FPD/FPI) controller is proposed for the secondary load frequency control (LFC) of a networked shipboard multi-microgrid (NSMMG). The effect of the various degradation factors associated with the communication infrastructure such as the time delay and packet loss is modeled and addressed to assess the system performance in the networked control system (NCS) operation. The parameters embedded in the established structure are decisive factors, which significantly affect the quality of control output actions. Accordingly, by employing the concepts of the black-hole optimization algorithm (BHA) and Lévy flight, an enhanced JAYA (EJAYA) algorithm is proposed to adjust the setting of the established structured controller. Finally, comprehensive studies and hardware-in-the-loop (HIL) real-time simulations are conducted to appraise the acceptability of the suggested controller for a secondary LFC problem in the face of the uncertain NCS.**

***Index Terms*—Secondary load frequency control (LFC), enhanced JAYA algorithm, networked shipboard multi-microgrid (NSMMG), 5G network technology.**

I. Introduction

DUE to the fuel consumption and gas emission rates of ships, which are extremely high; the integration of renewable energy sources (RESs) in power marine systems, as a special kind of the island microgrids (MGs), is constantly expanding [1]. The solar and sea wave energy resources are abundant on the oceans; as a result, the exploitation of RESs penetration could help to reduce the effect to the environment, increase energy conversion efficiency and fulfill other conventional power supply constraints such as security and reliability. However, some issues such as the intermittent and weather-dependent nature of RESs must be considered before RESs can become commonplace. Because of their stochastic characteristics, these technologies introduce power dips and power surges. A general shipboard microgrid can use energy storage systems (ESSs) such Battery Energy Storage System (BESS) and Flywheel Energy Storage System (FESS) to meet the remaining demand, when the energy of RESs is not sufficient [2-4].

M. Gheisarnejad is with Department of Electrical Engineering, Najafabad Branch, Islamic Azad University, Isfahan, Iran (e-mail: m.ghesar2@gmail.com).

M. H. Khooban is with the Department of Engineering, Aarhus University Denmark. (e-mail: mhkhoban@gmail.com, khooban@eng.au.dk).

T. Dragicevic, is with the Department of Energy Technology, Aalborg University, 9200 Aalborg, Denmark (e-mail: tdr@et.aau.dk).

Technically, a microgrid (MG) based shipboard is a cluster of distributed generators (DGs), ESSs and local loads, which are optimally planned for the profit of the customers. In [5, 6] the possible solutions of applying BESS in the marine industry are analyzed. A novel strategy is developed in [7] to find the optimal sizes for hybrid PV/diesel/ESS in a ship's power system. A critical literature review on the ship MGs has been reported in [8], where the different types of ESSs and various control methodologies have been studied. A hybrid non-integer fuzzy PD+I controller is proposed in [9] for the frequency fluctuation damping of an isolated shipboard MG. Matching of demand and supply, referred as the load frequency control (LFC), is vital to the reliable operation of integrating DGs and ESSs in the islanded microgrid. Some research works attempting to develop better the MG frequency control based on intelligent control [10], sliding mode control [11], model-predictive control [12], non-integer control [13] and adaptive-neuro [14].

Recently, network control system (NCS) for transmitting information among distributed system components (e.g. phasor measurement units (PMUs), controllers and actuators) have been increasingly used in the future microrids, since it exhibits a variety of benefits such as low installation cost, high speed, easy expansion and distributed management [15-17]. In the context of networked microgrids, there has been a few work devoted to this topic with various network technologies like Can bus [18], Ethernet [15, 19], ZigBee (IEEE 802.15.4) [18, 20], WiMax (IEEE 802.16) [21] and Wi-Fi (IEEE 802.11) [22], etc. Due to the bandwidth constraint in the communication network, taking advantage of the technologies is accompanied by network-induced delays and data packet dropouts. This circumstance seriously deteriorates the system performance and even threatens the reliability and stability if these unreliable factors are not properly handled during the control design. To deal with the challenges in the energy management of microgrids coupled with communication networks, there has been much less work research in the literature. For example, a discrete control strategy is proposed in [19] to compensate communication degradation and uncertainty conditions for the LFC of an MG. The authors have employed two communication architectures consist of Ethernet and hybrid network (Ethernet and 802.11b/g) for the integrated system and their performances are compared with a perfect communication as a benchmark. An event-triggered NCS scheme for robust L-infinity control is developed in [23] for a hybrid battery/wind in the form of MG. On the other hand, the application of Cellular Networks (e.g. CDMA, WCMDA, GSM, GPRS, 3G, LTE, 5G, etc.) in renewable energy solutions has become an emerging and highly appealing trend due to some benefits such as high capacity, low power usage, large information reliability, wide coverage

This article has been accepted for publication in a future issue of this journal, but has not been fully edited. Content may change prior to final publication. Citation information: DOI 10.1109/JESTPE.2019.2898854, IEEE Journal of Emerging and Selected Topics in Power Electronics

area, less interference from other signals [24, 25]. In this regard, the authors of [26] implemented the wireless internet connectivity for a interacted RESs to sends MG control center signals to PEV charge station. The application of the GPRS (General Packet Radio Service) and EGPRS (enhanced GPRS) standards is addressed in [27, 28] to send power reference information from the central control to wind power systems in a smart grid operation. The internet of things (IoT) based fifth generation (5G) is adopted in [29] for transmitting the observed information (measurement signals) of multiple-DERs to a control center.

The current study aims the application of 5G standards for the LFC of a shipboard unequal MMG considering the communication degradation. To implement proper LFC strategy in the NCS operation and for efficient utilization of the available RESs, a new interval type-2 fractional order fuzzy PD/fuzzy PI (IT2FO-FPD/FPI) controller, in discrete form, is employed for the aforesaid system. For this purpose, the concepts of BHA and levy flight are followed to avoid the weakness of falling into local optimum and to enhance the global searching ability of a recently developed JAYA algorithm [30]. Then, the enhanced JAYA (EJAYA) algorithm is adopted to simultaneously adjust the decisive coefficients embedded in the hybrid structure of the IT2FLC and FO operators. The contributions of the suggested framework can be listed as follows:

1. A new optimal based fuzzy controller with fractional order gains is established for the secondary LFC in the networked shipboard MMG,
2. Since the system performance depends on the fine-tuning of controller parameters to function successfully, the parameters of the suggested controller are adjusted by a new version of JAYA algorithm to obtain an optimal performance,
3. In particular, the 5G network technology is employed as the communication infrastructure in the concerned NCS system,
4. The effects of network degradations (i.e. time delay and packet loss) are studied in the small-signal modelling of the NCS system, as these degradations are occurred in the realistic communication networks,
5. The suggested technique is implemented and validated in a real-time NSMMG system testbed using hardware-in-the-loop (HIL) simulator to investigate its testbed applicability from a systemic perspective.

The remainder of this work is organized as follows: the model of the NSMMG system with network communication descriptions is presented in Section II. The proposed structured IT2FO-FPD/FPI controller is also described in Section II. The enhanced version of the JAYA algorithm (EJAYA) is developed in Section III. The contribution of the suggested framework is elaborated in Section IV. The conclusion of this work is given in Section V. The simulation results along with the related discussions are presented in Section V. Lastly, the conclusion of this paper is drawn in Section VI.

II. STUDY SYSTEM AND MODELING

The structure of the concerned NSMMG system is illustrated in Fig. 1, where 5G technology with the binary phase shift keying (BPSK) is adopted as the networking infrastructure. The data rate of the shared network is chosen as 2 Gbps. The simulation of the MMG power system is carried out by considering continuous time model while the controller is discrete, since PMUs send periodically measured packets to the control center. In the future shipboard power system, the control center sends the control signals to diesel ship generator (DSG) and energy storage units (BESS and FESS) wirelessly. According to Fig. 1, there are three controllers, where area control errors (ACE) and frequency grid deviation (Δf) are measured by PMUs each 0.01 s and transmitted to their respective control center via the shared communication. The parameters of the concerned MMG system, depicted in Fig. 1, are listed in Table. I.

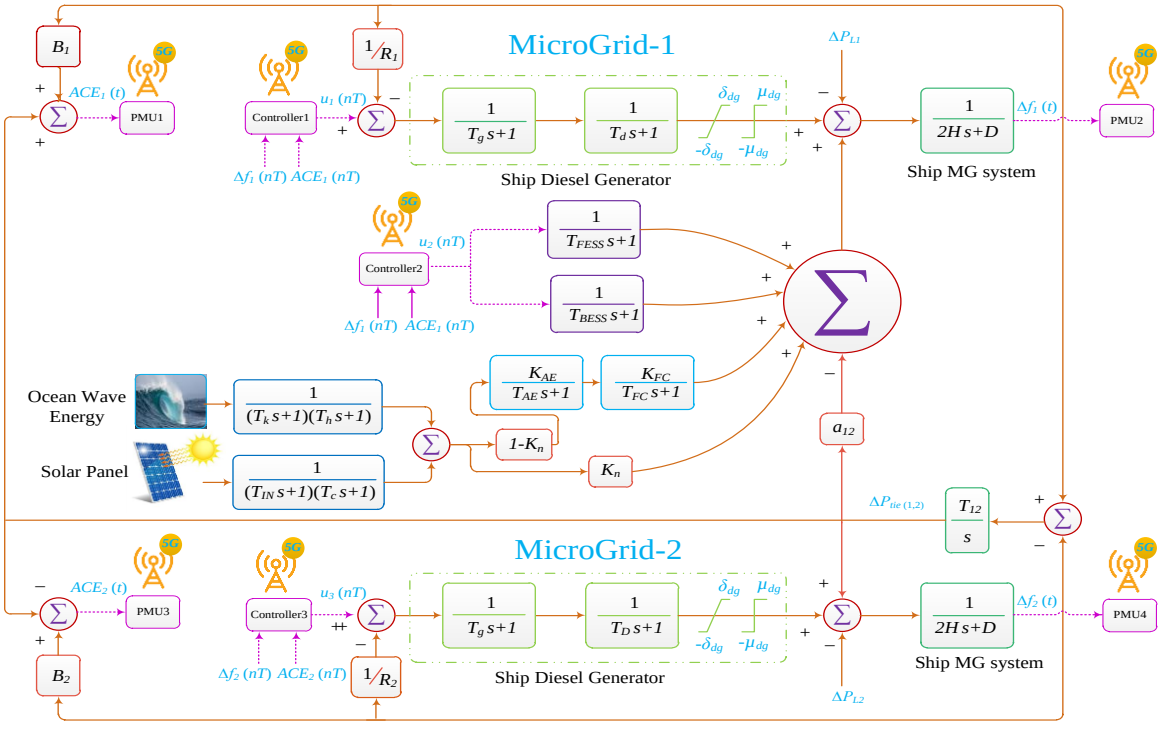

Fig. 1. The overall shipboard multi microgrid scheme over 5G network.

This article has been accepted for publication in a future issue of this journal, but has not been fully edited. Content may change prior to final publication. Citation information: DOI 10.1109/JESTPE.2019.2898854, IEEE Journal of Emerging and Selected Topics in Power Electronics

Table I: MMG power system's parameters [9]

Symbol and Abbreviation	Values	Symbol and Abbreviation	Values
T_g (governor time constant)	2.000 s	T_{FESS}	0.1 s
T_d (diesel generator time constant)	1.000 s	T_{BESS}	0.1 s
R_1, R_2 (DG speed regulations)	3.000	T_{In}	4 s
B_1, B_2 (frequency bias constant)	0.9	T_c	0.5 s
δ_{dg} (ramp rate limits)	0.01	T_G	0.5 s
μ_{dg} (power increment)	0.025	T_h	4 s
D (damping coefficient)	0.012	T_{FC}	4.000 s
$2H$ (inertia constant)	0.2	T_{AE}	0.5 s
K_{FC}	1/50	T_{12}	0.2
K_n	0.6	a_{12}	-1

A. The shipboard MMG system

In the present work, a load frequency control in the shipboard MMG is investigated, which consists of two MGs connected by tie-lines as illustrated in Fig. 2. The MG-1 comprises of a set of different Distributed Generations such as SWE, PV, DSG, FC system and energy storage units like BESS and FESS, while the only DSG unit is considered in the MG-2. The PV, Fuel Cell (FC), BESS and FESS units are linked to the AC MG via DC/AC interfacing inverters. The FC model is described by a third-order transfer function [10, 31]. To prevent the effects of disturbances or for maintaining control objectives, a circuit breaker is employed to link micro sources to the AC bus. The DSG power system is established for the spinning reserve of the secondary frequency control.

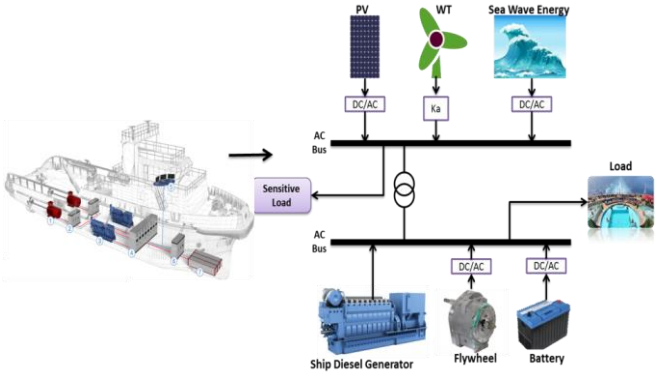

Fig. 2. The case study for the LFC in a shipboard MG.

B. Model of Unreliable Communication Network

Fig. 3 depicts a simplified representation of the NSMMG system, which can be classified into the following five components: the controlled MMG, the PMU, the actuator, controller and the unreliable 5G communication network under the network degradation factors.

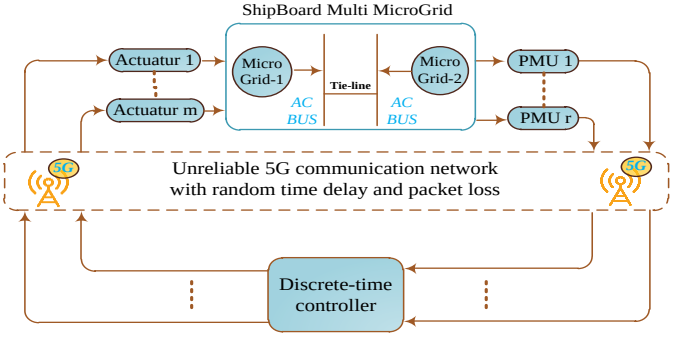

Fig. 3. Structure of the 5G networked Shipboard MMG.

The specifications of the applied degradation factors (shown in Fig. 3) are presented in the following.

The advent of the communication network in various applications will inevitably lead to the time delay in sending and receiving of data packets [32, 33]. Time delays in the NCS operation can be classified into two types: data time delay between PMU (sensor) to controller center τ^{sc} and data time delay between controller center to actuator τ^{ca}. In the present simulation, τ^{sc} and τ^{ca} entered into the shared network.

The second source of disturbance that has a significant impact on network degradation lies at the packet loss [19, 34]. The degradation factor exists in the forward and feedback channel of the wireless networks, which can be modeled as a binary two-state switch. In this study, a Bernoulli distribution [19] with the stochastic variable θ_k is considered as:

$$Pr\{\theta_k = 0\} = \alpha_{lp} \tag{1}$$

where $\theta_k \epsilon \{0, 1\}$, $\theta_k = 0$ indicates the occurrence of packet loss, $\theta_k = 1$ means there is no packet loss and $0 < \alpha_{lp} < 1$ is the specified packet loss probability.

C. Discrete IT2FO-FPD/FPI controller

FO operators integration/differentiation have additional freedom in control design, which this improves the efficiency and robustness. The utilization of the operators is more beneficial when they are combined with the FLCs in the effective structures [35]. Fig. 4 shows a general structure of IT2FO-FPD/FPI controller, inherited from IT2FO-FPD and IT2FO-FPI controllers, which is comprehensively discussed in [35]. In Fig. 4, G_E^{PD}, G_{CE}^{PD}, G_u^{PD}, μ_{PD}, G_E^{PI}, G_{CE}^{PI}, G_u^{PI}, μ_{PI} and λ_{PI} are decisive parameters in the realization of a well-behaved controller.

Here, the binomial expansion of the backward difference method is used to approximate FO operators [36]. According to Fig. 4, the control laws of the IT2FO-FPD and IT2FO-FPI controllers are described in Eqs. (2) and (3), respectively.

$$G_E^{PD} e(nT) + G_{CE}^{PD}\left(D^{\mu_{PD}}(e(nT))\right) = G_u^{PD} u_{PD}(nT) \tag{2}$$

$$G_E^{PI} y(nT) + G_{CE}^{PI}\left(D^{\mu_{PI}}(y(nT))\right) = G_u^{PI}\left(D^{-\lambda_{PI}}(\Delta u_{PI}(nT))\right) \tag{3}$$

Therefore, the output of an IT2FO-FPD/FPI controller is obtained as:

$$u_{IT2FO-FPD/FPI}(nT) = G_u^{PD} u_{PD}(nT) + G_u^{PI}\left(D^{-\lambda_{PI}}(\Delta u_{PI}(nT))\right) \tag{4}$$

In the present study, due to a fact that triangular membership functions (MFs) are very simple to apply in practical hardware, this kind of MFs are chosen for IT2FLCs/T1FLCs as implemented in [37]. The universe of discourse is considered to be [-1 1] for error and fractional derivative of error. The antecedent MFs for both input and output variables are including, NL (negative large), NS (negative small), Z (zero), PS (positive small) and PL (positive large). The optimal executed IT2FLSs/T1FLCs rules are written in Table II. Moreover, the COS type reduction and centroid defuzzification method are utilized for the IT2FLCs and the T1FLCs, respectively, and product type operator is utilized for implication in both FLCs.

This article has been accepted for publication in a future issue of this journal, but has not been fully edited. Content may change prior to final publication. Citation information: DOI 10.1109/JESTPE.2019.2898854, IEEE Journal of Emerging and Selected Topics in Power Electronics

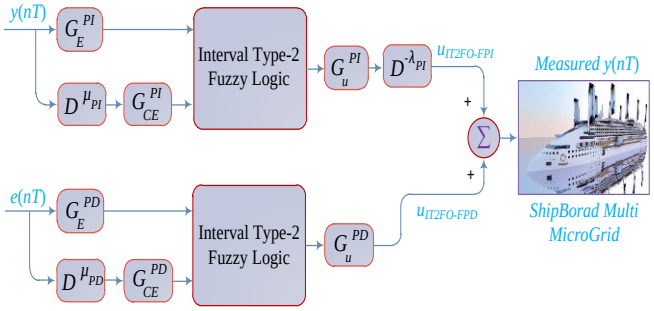

Fig. 4. The general scheme of IT2FO-FPD/FPI

Table II. The IT2FLCs/T1FLCs Rules Set

e \ ė	NL	NS	Z	PS	PL
NL	NL	NL	NL	NS	Z
NS	NL	NL	NS	Z	PS
Z	NL	NS	Z	PS	PL
PS	NS	Z	PS	PL	PL
PL	Z	PS	PL	PL	PL

D. Fractional order operator

Fractional calculus (FC) is the generalization of integer order integration/differentiation to any arbitrary real number. Among the various definitions found in literature, the Grünwald-Letnikov (G-L) is frequently employed in realizing the FC concepts in control theory [38]. The G-L definition is written as:

$$ {}_aD_t^{\alpha} f(t) = \lim_{h\to 0} \frac{1}{h^{\alpha}} \sum_{k=0}^{\left[\frac{t-a}{h}\right]} (-1)^k \binom{\alpha}{k} f(t-kh) \tag{5} $$

where a, t is the bounds, α is the is the order of the operation and $\binom{\alpha}{k} = \frac{(\alpha)(\alpha-1)(\alpha-2)\ldots\ldots(\alpha-k+1)}{\Gamma(k-1)}$.

To implement a discrete time version of the established controller, a discrete definition of G-L is required. Utilizing the backward difference method $s = (1-z^{-1})/T$, where T is sampling period, the FO operators can be discretized as expressed in the following equation [36]:

$$ D^{\alpha}(f[n]) = T^{-\alpha} \sum_{k=0}^{\infty} d_k f[n-k] \tag{6} $$

where the coefficient d_k can be expressed by the following recursive algorithm.

$$ d_k = (1-(1+\alpha)/k) d_{k-1}; k = 1,2,\ldots; d_0 = 1 \tag{7} $$

E. Basic concept of type-2 fuzzy sets

An interval type-2 fuzzy set (IT2FS) $\tilde{A}$ is defined as [37, 39]:

$$ \tilde{A} = \int_{x\,\epsilon\,X} \int_{v\,\epsilon\,J_x \subseteq [0,1]} 1/(x,v) = \int_{x\,\epsilon\,X} \left[\int_{v\,\epsilon\,J_x \subseteq [0,1]} 1/(x,v) \right] /x \tag{8} $$

where x denotes the primary variable and $x\,\epsilon\,X$; v denotes the secondary variable, $v\,\epsilon\,V$ which has a domain J_x at each $x\,\epsilon\,X$; J_x represents the membership of x as described in Eq. (12). The union of all the primary memberships (i.e. Uncertainty about $\tilde{A}$) is known as the foot print of uncertainty (FOU):

$$ FOU\,(\tilde{A}) = \bigcup_{\forall\, x\,\epsilon\,X} J_x = \{(x,v) : v\,\epsilon\, J_x \subseteq [0,1]\} \tag{9} $$

The FOU of IT2FS is bonded by two type-1 MFs. The upper bound of FOU ($\tilde{A}$) is represented as $\overline{\mu}_{\tilde{A}}(x)$ and lower bound of FOU ($\tilde{A}$) is represented as $\underline{\mu}_{\tilde{A}}(x)$, $\forall\, x\,\epsilon\, X$:

$$ \overline{\mu}_{\tilde{A}}(x) = \overline{FOU\,(\tilde{A})} \quad \forall\, x\,\epsilon\, X \tag{10} $$

$$ \underline{\mu}_{\tilde{A}}(x) = \underline{FOU\,(\tilde{A})} \quad \forall\, x\,\epsilon\, X \tag{11} $$

Note that J_x is an interval set:

$$ J_x = \{(x,v) : v\,[\underline{\mu}_{\tilde{A}}(x),\ \overline{\mu}_{\tilde{A}}(x)]\} \tag{12} $$

F. Interval type-2 fuzzy logic system

The IT2FLC, as an extension of type-1 fuzzy logic controller (T1FLC), is designed with the concept of type-2 fuzzy logic sets (T2FLSs). The generic rule structure of IT2FLC with N rule is as:

$$ R_n: \text{if } x_1 \text{ is } \tilde{F}_{1,n} \text{and} \ldots x_i \text{ is } \tilde{F}_{i,n} \ldots \text{and} x_I \text{ is } \tilde{F}_{I,n}, \text{Then } y \text{ is } \tilde{Y}_n \tag{13} $$

where n=1, 2, … ,N, $\tilde{F}_{i,n}(i = 1,2,\ldots I)$ are the antecedent MFs, $Y_n = [\underline{y}_n\ \overline{y}_n]$ represents the consequent MFs.

Suppose $x' = (x_1', x_2', \ldots, x_I')$ is a crisp input vector. The steps of the output calculations in an IT2FLS are as follows [37]:

Step 1: The antecedent IT2MFs can be defined in terms of lower MF ($\underline{\mu}_{\tilde{F}_n}$) and upper MF ($\overline{\mu}_{\tilde{F}_n}$).

Step 2: The total firing strength for the n^{th} rule is as:

$$ F_n(x') = \left[\underline{\mu}_{\tilde{F}_{1,n}}(x_1') * \ldots * \underline{\mu}_{\tilde{F}_{I,n}}(x_I'), \overline{\mu}_{\tilde{F}_{1,n}}(x_1') * \ldots * \overline{\mu}_{\tilde{F}_{I,n}}(x_I')\right] = \left[\underline{f}_n, \overline{f}_n\right]\ n = 1, \ldots, N \tag{14} $$

Step 3: Type-reduction is employed to combine $F_n(x')$ and the related rule consequences.

Step 4: The defuzzified crisp output of an IT2FLS is obtained as $y = (y_r + y_l)/2$. Where y_r and y_l are the end points of the type reduced set which are computed as:

$$ y_l = \frac{\sum_{n=1}^{L} \underline{y}_n \overline{f}_n + \sum_{n=L+1}^{N} \underline{y}_n \underline{f}_n}{\sum_{n=1}^{L} \overline{f}_n + \sum_{n=L+1}^{N} \underline{f}_n} \tag{15} $$

$$ y_r = \frac{\sum_{n=1}^{R} \overline{y}_n \underline{f}_n + \sum_{n=R+1}^{N} \overline{y}_n \overline{f}_n}{\sum_{n=1}^{R} \underline{f}_n + \sum_{n=R+1}^{N} \overline{f}_n} \tag{16} $$

In above Eqs. (15) and (16), the switching points (L, R) can be calculated via the Karnik–Mendel (KM) type-reduction method.

III. Proposed Controller and Objective Function

JAYA is a newly developed meta-heuristic algorithm, which has shown excellent feasibility to solve engineering optimization problems [30, 40] since it is free from any key parameter settings. In the algorithm, the solutions are updated through attaining the best solution and moving away from the worst solution as formulated in Eq. (17).

$$ Y_i^k = y_i^k + rand()\left(y_b^k - \left|y_i^k\right|\right) - rand()\left(y_w^k - \left|y_i^k\right|\right) \tag{17} $$

where Y_i^k is the modified solution of y_i^k during kth iteration; y_b^k and y_w^k are the best and worst values achieved until the kth iteration.

This article has been accepted for publication in a future issue of this journal, but has not been fully edited. Content may change prior to final publication. Citation information: DOI 10.1109/JESTPE.2019.2898854, IEEE Journal of Emerging and Selected Topics in Power Electronics

A. Enhanced JAYA based BHA and Lévy flight

Owing to the original JAYA benefits the distance between best and worst individuals to global search, the exploitation outperforms exploration in the final generations, which this increase the trapping into a local optimum. To overcome the weakness, initially, the updating mechanism of original JAYA is improved by black-hole algorithm concept. According to the strategy, when the distance between a candidate's individual and best solution is less than the radius of the event horizon (R) during the updating process of JAYA, a new candidate is randomly generated. The value R is calculated as [41]:

$$R = \frac{y_b}{\sum_{i=1}^{k} y_i} \tag{18}$$

Moreover, to avoid diversity loss of JAYA, a novel updating mechanism with Lévy-based motion, as another modification, is proposed in Eq. (19).

$$Y_i^k = y_i^k + rand()\left(y_b^k - \left|y_i^k\right|\right) - rand()\left(y_w^k - \left|y_i^k\right|\right) + rand()\; y_i^k \times Lévy(\beta) \tag{19}$$

where Lévy(β) generate a random walk, in which the random-steps are generated based on the Lévy distribution [42].

$$Lévy(\beta) \sim u = t^{-\beta} \tag{20}$$

The pseudo-code of the EJAYA is illustrated in Algorithm 1.

Algorithm 1: The pseudo-code of EJAYA algorithm.

I. *Set the algorithm parameters, Initialize a random population*
II. ***while*** *gen=1 to Max-Gen* ***do***
III. ***for*** *i=1* ***to*** *Population size* ***do***
IV. *Identify the best and worst solutions in the population*
V. ***If1*** *rand < 1/2* ***then***
VI. *Update the solutions by the original JAYA algorithm*
VII. *Calculate R using Eq. (18)*
VIII. $D_i = \sqrt{(y_1 - y_b)^2 + \cdots + (y_N - y_b)^2}$
IX. ***If2*** $D_i < R$ ***then***
X. $y_i \leftarrow$ *Randomly generate individual*
XI. ***end if2***
XII. ***else1***
XIII. *Update the solutions by the Eq. (19)*
XIV. ***end if1***
XV. ***end for***
XVI. *Check limitations and repair the solutions if they are violated from boundary constraints*
XVII. ***for*** *i=1 to Population size* ***do***
XVIII. ***if*** $f(Y_i) < f(y_i)$ ***then*** *Replace* y_i *with* Y_i ***end*** *if*
XIX. ***end for***
XX. *Report the optimum solution*
XXI. ***end while***

The LFC objectives in the NSMMG are fulfilled by measuring Δf and ΔP_{tie}. For the optimum setting of the LFC controller, the objective function is chosen as defined in Eq. (21) [42].

$$J = \int_0^{90} \left[B_1^2 {\Delta f_1}^2 + B_2^2 {\Delta f_2}^2 + {\Delta P_{tie}}^2\right] \tag{21}$$

IV. The Contributions of the Proposed Study

To sum up, the main novelties of the paper can be summarized as follows:

1. The suggested novel control approach is easy to implement and can be utilized for a reasonably wide class of shipboard and other types of MGs.
2. For the first time, the 5G network technology is applied for the secondary LFC in the shipboard MG.
3. The suggested novel control signals are based only on the available plant input/output information and can be calculated online.
4. Another advantage of the suggested control technique is its light burden of computations, which is an important feature in the practical implementation and online control cases.
5. The OPAL-RT real-time simulator is applied to examine the performance and robustness of the new suggested controller over the time delay.

V. Simulation and Experimental Results

In this section, for the evaluation of the proposed control strategy, the 5G wireless network applied to the shipboard MMG (shown in Fig. 1) is simulated in MATLAB/Simulink software. To verify the advantages of the suggested controller, the case study is also examined with the T1FO-FPD/FPI [35], model-free SMC [43] and conventional PD/PI controllers. Since the controller output depends on the design parameters, the EJAYA is executed for optimal computation of the parameters embedded into the different controllers. In order to assess the performance of the proposed control strategy in the context of the NSMMG depicted in Fig. 1, the Hardware-In-the Loop (HIL) real time simulation approach is implemented. The real time HIL method is used to emulate errors and delays that do not exist in the classical off-line simulations. Fig. 5 sketches the HIL setup, and for more details about the components of this setup: readers are referred to [44].

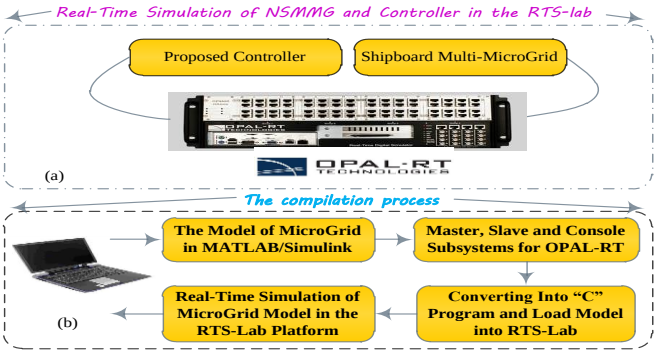

Fig.5.The real-time experimental setup. (a) the real-time simulation of NSMMG and controller in the RTS-LB, (b) the compilation process.

A. Specifications for the shiboared multi-microgrid

In the integrated system, the multi-step load variation is considered as generic disturbances in both the MGs (See Fig. 6) simultaneously. Additionally, the stochastic power fluctuations of the SWE (ΔP_{SWE}) and PV (ΔP_{pv}) is applied to the LFC (See Fig. 7). The sea wave energy data, which is extracted from the National Oceanographic Data Center [45] is depicted in Fig. 7a, while Fig. 7b exhibits the solar radiation data in Aberdeen (United Kingdom) [46].

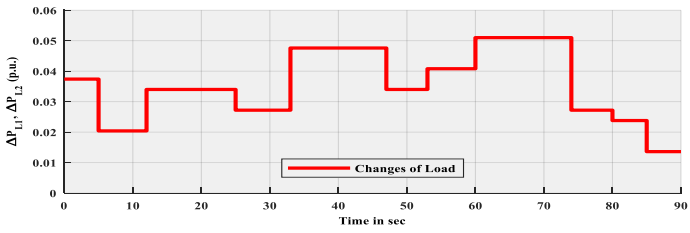

Fig. 6. Step changes of the load in the time interval of 90 seconds.

This article has been accepted for publication in a future issue of this journal, but has not been fully edited. Content may change prior to final publication. Citation information: DOI 10.1109/JESTPE.2019.2898854, IEEE Journal of Emerging and Selected Topics in Power Electronics

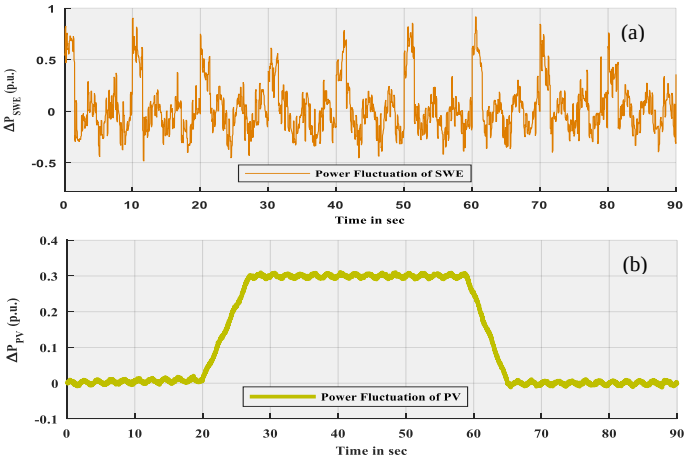

Fig. 7. Power fluctuations, (a) SWE, (b)- PV.

B. Effect of time delay and packet loss

The effect of time delay in the interval [10ms 100ms] on the concerned NSMMG system is investigated, when packet loss is set to 15 %. Fig. 8 illustrates the performance comparison of the designed controllers. As observed, IT2FO-FPD/FPI controller provides a smaller fitness value ($J(21)$) in the presence of different time delays than other controllers. Based on [25], establishing 5G in the integrated power systems demand a time delay in the order of 1–100 ms. Therefore, the IT2FO-FPD/FPI controller is effective to restore system frequency against different time delays in the NCS operation.

Next, the Bernoulli distribution with different loss probability and time delay 50 ms is considered to evaluate the effect of packet loss on the NSMMG system. The performance measure values computed for the different controllers are presented in Fig. 9. It is evident that the effect of packet loss on the compared controllers is insignificant for $\alpha_{LP} \leq 0.25$. The fitness value of the different controllers are significantly increased for $\alpha_{LP} > 0.3$; however, they still provide a small fitness value to ensure the efficient frequency deviation damping. So, the designed controllers realize the LFC requirements of networked integrated systems in the presence of large packet losses. It is also observed that a minimum fitness value is obtained by the IT2FO-FPD/FPI controller than other controllers for different values of the packet losses. Hence, it can be concluded that the suggested controller improves the stability of LFC of the NSMMG system when the packet losses are considered in the shared network.

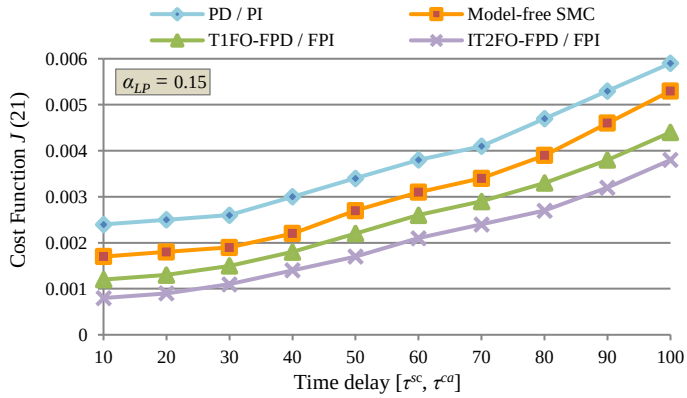

Fig. 8. Performance comparison with different time delays under α_{LP} = 0.15.

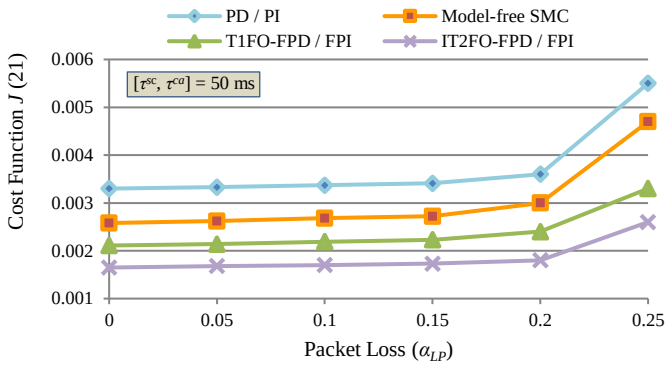

Fig. 9. Performance comparison with various different packet loss under time delay 50 ms.

C. Dynamic performances in the presence of RESs

To study the performance of the NSMMG system against the communication degradation effects, the network delays (τ^{sc} and τ^{ca}) are assumed to be 50 ms and the probability of the packet loss in the network is α_{lp}=0.15. Fig. 10 depicts the output of the frequency deviation of MG-1 in the presence of RESs. It is explicitly noted from Fig. 10 in spite of having high system complexity, such as stochastic fluctuations of RESs and the network communication degradation; all the designed NSMMG secondary controllers are robust enough to stabilize the system. It is also found that by adopting IT2FO-FPD/FPI controller, the transient curves are settled down in a less time with further diminished fluctuations in comparison to the structured T1FO- FPD/FPI, model-free SMC and PD/PI controllers. Thus, it can be inferred that the dynamic behavior of the network control system is improved with the proposed technique. The powers generated by the controlled FESS and BESS are painted in Fig. 11. It is evident that with the IT2FO-FPD/FPI controller, the response fluctuations of the energy storage systems are further suppressed in comparison with other three controllers. This implies that if the proposed technique is used, there is less need for charging/discharging the batteries to alleviate the grid frequency fluctuations which leads to increase the lifetime of the ESSs. This makes the NSMMG system more efficient from the health and economics point of the view.

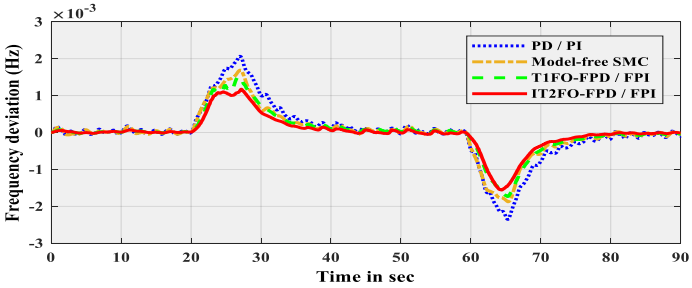

Fig. 10. Frequency deviation in MG-1 in the presence of RESs.

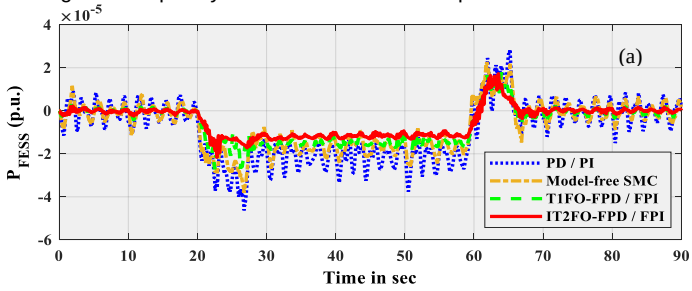

This article has been accepted for publication in a future issue of this journal, but has not been fully edited. Content may change prior to final publication. Citation information: DOI 10.1109/JESTPE.2019.2898854, IEEE Journal of Emerging and Selected Topics in Power Electronics

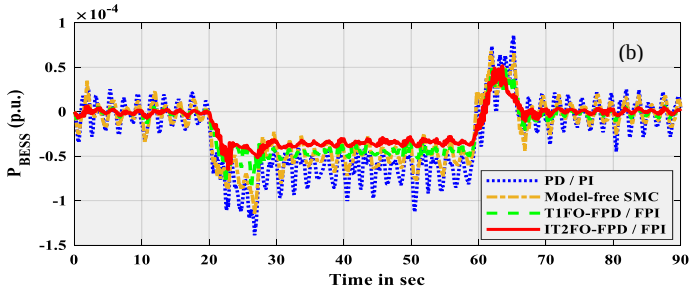

Fig. 11. The output power of storage energy systems in the presence of RESs, (a) FESS, (b) BESS.

D. Dynamic performances in the presence of RESs and load demand

In this section, the multi-step load variation is also considered in the NSMMG system. The curves of frequency deviation in the MG-1 for each controller are plotted in Fig. 12, where the time delay and packet loss probability are set as 50ms and 0.15, respectively. It is observed that with the suggested structured IT2FO-FPD/FPI controller, the NCS system is faster to restore the frequency oscillations in comparison with the T1FO- FPD/FPI, model-free SMC and PD/PI controllers. The outputs of the controllable storage devices (i.e. FESS and BESS) are depicted in Fig. 13. The features of storage devices outputs shown in Fig. 13 reveal that more desirable qualification in the outputs is achievable by adopting the suggested controller where the overshoots of the oscillations are further restored than the other considered controllers.

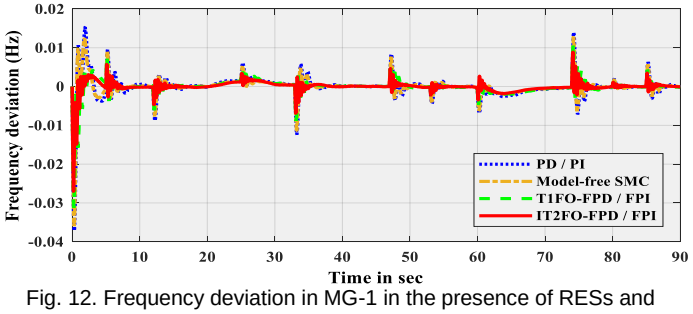

Fig. 12. Frequency deviation in MG-1 in the presence of RESs and load demand.

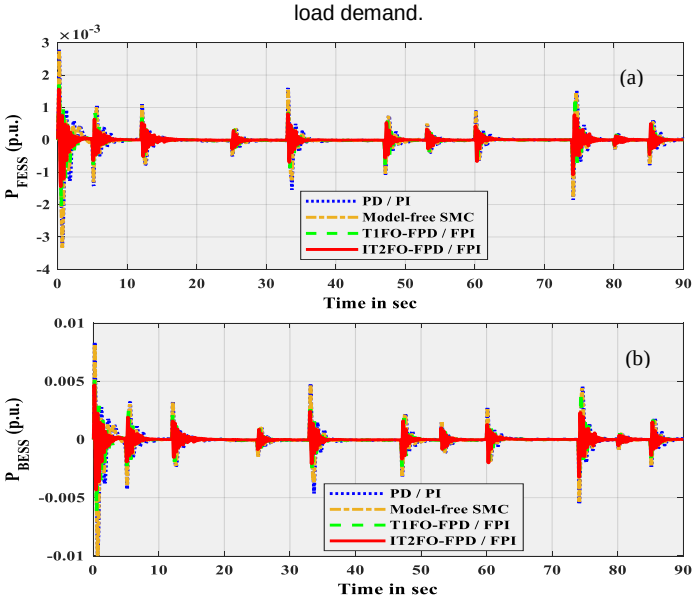

Fig. 13. The output power of storage energy systems in the presence of RESs and load demand, (a) FESS, (b) BESS.

E. Robustness analysis

The robustness of the designed controller based LFC operations subjected to both the physical parameters and communication degradation factors is studied in this section. The parameters variations of the scenario are as follows: T_g = +30%; T_d = -25%; D = +20%; H = -30%; T_{FESS} = +25%; T_{BESS} = -35% (for physical parameters) and $\tau^{sc} = \tau^{ca}$ = -0.20%; α_{lp} = +30% (for communication degradation factors). It is notable that the parameters variations are much harder to handle and each variation of them may cause system instability. Fig. 14 reveals the abilities of the concerned controllers for unknown network configurations. It is viewed from Fig. 14 that the suggested controller is high-performing and effectively handles the aforesaid scenario and result in small frequency fluctuations. Moreover, it is observed that the IT2FO-FPD/FPI controller is less sensitivity dealing with a more severe changing of the system parameters than the T1-FPD/FPI, model-free SMC and PD/PI controllers. Thus, it can be inferred that the proposed controller provides a higher degree of robustness performance compared to the other considered controllers.

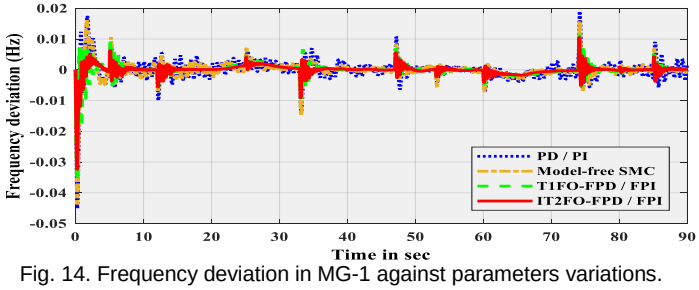

Fig. 14. Frequency deviation in MG-1 against parameters variations.

VI. CONCLUSION

In particular, this framework focused on a networked shipboard MMG, and allows investigating both aspects of physical disturbances (i.e. load variation and intermittent behavior of the SWE and PV) and network degradations (i.e. time delay and packet loss). In the study, a novel intelligent IT2FO-FPD/FPI controller based on an enhanced version of the JAYA algorithm, named EJAYA, is proposed for the LFC problem in a smart grid operation. The PMUs measurements and control signals were transmitted via the shared communication network by employing the future 5G technology. The experimental simulation reveals that the proposed technique improves the stability of the interconnected microgrids and outperforms other comparative techniques. Furthermore, to ascertain the efficiency and robustness of the suggested framework, unknown configurations of network degradation are accomplished. The superiority of IT2FO-FPD/FPI controller was confirmed as compared to other techniques.

References

[1] F. Shariatzadeh, N. Kumar, and A. K. Srivastava, "Optimal control algorithms for reconfiguration of shipboard microgrid distribution system using intelligent techniques," *IEEE Transactions on Industry Applications*, vol. 53, pp. 474-482, 2017.

[2] B. Fan, C. Wang, Q. Yang, W. Liu, and G. Wang, "Performance guaranteed control of flywheel energy storage system for pulsed power load accommodation," *IEEE Trans. Power Syst.*, 2017.

[3] J. Hou, J. Sun, and H. F. Hofmann, "Mitigating power fluctuations in electric ship propulsion with hybrid energy storage system: Design and analysis," *IEEE Journal of Oceanic Engineering*, 2017.

[4] R. Heydari, M. Gheisarnejad, M. H. Khooban, T. Dragicevic, and F. Blaabjerg, "Robust and Fast Voltage-Source-Converter (VSC) Control for Naval Shipboard Microgrids," *IEEE Transactions on Power Electronics*, 2019. DOI: 10.1109/TPEL.2019.2896244

[5] G. S. Misyris, A. Marinopoulos, D. I. Doukas, T. Tengnér, and D. P. Labridis, "On battery state estimation algorithms for electric ship applications," *Electric Power Systems Research*, vol. 151, pp. 115-124, 2017.

[6] K. Kim, K. Park, J. Ahn, G. Roh, and K. Chun, "A study on applicability of Battery Energy Storage System (BESS) for electric propulsion ships," pp. 203-207.

[7] H. Lan, S. Wen, Y.-Y. Hong, C. Y. David, and L. Zhang, "Optimal sizing of hybrid PV/diesel/battery in ship power system," *Applied energy*, vol. 158, pp. 26-34, 2015.

[8] S. G. Jayasinghe, L. Meegahapola, N. Fernando, Z. Jin, and J. M. Guerrero, "Review of ship microgrids: System architectures, storage technologies and power quality aspects," *Inventions*, vol. 2, p. 4, 2017.

[9] M.-H. Khooban, T. Dragicevic, F. Blaabjerg, and M. Delimar, "Shipboard microgrids: a novel approach to load frequency control," *IEEE Transactions on Sustainable Energy*, vol. 9, pp. 843-852, 2018.

[10] A. Modirkhazeni, O. N. Almasi, and M. H. Khooban, "Improved frequency dynamic in isolated hybrid power system using an intelligent method," *International Journal of Electrical Power & Energy Systems*, vol. 78, pp. 225–238, Jun. 2016.

[11] F. Valenciaga and P. F. Puleston, "High-order sliding control for a wind energy conversion system based on a permanent magnet synchronous generator," *IEEE transactions on energy conversion*, vol. 23, pp. 860-867, 2008.

[12] J. Pahasa and I. Ngamroo, "Coordinated Control of Wind Turbine Blade Pitch Angle and PHEVs Using MPCs for Load Frequency Control of Microgrid," *IEEE Systems Journal*, vol. 10, pp. 97-105, 2016.

[13] M.-H. Khooban, T. Niknam, M. Shasadeghi, T. Dragicevic, and F. Blaabjerg, "Load Frequency Control in Microgrids Based on a Stochastic Noninteger Controller," *IEEE Transactions on Sustainable Energy*, vol. 9, no. 2, pp. 853–861, Apr. 2018.

[14] F. Hafiz and A. Abdennour, "An adaptive neuro-fuzzy inertia controller for variable-speed wind turbines," *Renewable Energy*, vol. 92, pp. 136-146, 2016.

[15] V. P. Singh, N. Kishor, and P. Samuel, "Load frequency control with communication topology changes in smart grid," *IEEE Transactions on Industrial Informatics*, vol. 12, pp. 1943-1952, 2016.

[16] Y. Yan, Y. Qian, H. Sharif, and D. Tipper, "A survey on smart grid communication infrastructures: Motivations, requirements and challenges," *IEEE communications surveys & tutorials*, vol. 15, pp. 5-20, 2013.

[17] S. Liu, P. X. Liu, and X. Wang, "Stability analysis and compensation of network-induced delays in communication-based power system control: A survey," *ISA transactions*, vol. 66, pp. 143-153, 2017.

[18] A. Alfergani, A. Khalil, and Z. Rajab, "Networked control of AC microgrid," *Sustainable cities and society*, vol. 37, pp. 371-387, 2018.

[19] H. Mo and G. Sansavini, "Real-time coordination of distributed energy resources for frequency control in microgrids with unreliable communication," *International Journal of Electrical Power & Energy Systems*, vol. 96, pp. 86-105, 2018.

[20] N. C. Batista, R. Melício, J. C. O. Matias, and J. P. S. Catalão, "Photovoltaic and wind energy systems monitoring and building/home energy management using ZigBee devices within a smart grid," *Energy*, vol. 49, pp. 306-315, 2013.

[21] M. M. Eissa, "New protection principle for smart grid with renewable energy sources integration using WiMAX centralized scheduling technology," *International Journal of Electrical Power & Energy Systems*, vol. 97, pp. 372-384, 2018.

[22] L. K. Siow, P. L. So, H. B. Gooi, F. L. Luo, C. J. Gajanayake, and Q. N. Vo, "Wi-Fi based server in microgrid energy management system," pp. 1-5.

[23] J. Sun, Y. Hu, Y. Chai, R. Ling, H. Zheng, G. Wang, *et al.*, "L-infinity event-triggered networked control under time-varying communication delay with communication cost reduction," *Journal of the Franklin Institute*, vol. 352, pp. 4776-4800, 2015.

[24] Y. Saleem, N. Crespi, M. H. Rehmani, and R. Copeland, "Internet of things-aided Smart Grid: technologies, architectures, applications, prototypes, and future research directions," *arXiv preprint arXiv:1704.08977*, 2017.

[25] I. Parvez, A. Rahmati, I. Guvenc, A. I. Sarwat, and H. Dai, "A survey on low latency towards 5G: RAN, core network and caching solutions," *IEEE Communications Surveys & Tutorials*, 2018.

[26] A. Khalil, Z. Rajab, A. Alfergani, and O. Mohamed, "The impact of the time delay on the load frequency control system in microgrid with plug-in-electric vehicles," *Sustainable Cities and Society*, vol. 35, pp. 365-377, 2017.

[27] C. M. Rocha-Osorio, J. S. Solís-Chaves, I. R. S. Casella, C. E. Capovilla, J. L. A. Puma, and A. J. Sguarezi Filho, "GPRS/EGPRS standards applied to DTC of a DFIG using fuzzy–PI controllers," *International Journal of Electrical Power & Energy Systems*, vol. 93, pp. 365-373, 2017.

[28] J. G. Cardoso, I. R. S. Casella, C. E. Capovilla, and A. J. Sguarezi Filho, "Comparison of wireless power controllers for induction aerogenerators connected to a smart grid based on GPRS and EGPRS standards," *Journal of Control, Automation and Electrical Systems*, vol. 27, pp. 328-338, 2016.

[29] M. Rana, L. Li, and S. Su, "Kalman filter based microgrid state estimation and control using the IoT with 5G networks."

[30] R. Rao, "Jaya: A simple and new optimization algorithm for solving constrained and unconstrained optimization problems," *International Journal of Industrial Engineering Computations*, vol. 7, pp. 19-34, 2016.

[31] D.-J. Lee and L. Wang, "Small-signal stability analysis of an autonomous hybrid renewable energy power generation/energy storage system part I: Time-domain simulations," *IEEE Transactions on Energy Conversion*, vol. 23, pp. 311-320, 2008.

[32] N. Vafamand, M. H. Khooban, T. Dragičević, and F. Blaabjerg, "Networked fuzzy predictive control of power buffers for dynamic stabilization of DC microgrids," *IEEE Transactions on Industrial Electronics*, vol. 66, pp. 1356-1362, 2019.

[33] I. Pan and S. Das, "Fractional order AGC for distributed energy resources using robust optimization," *IEEE Transactions on Smart Grid*, vol. 7, pp. 2175-2186, 2016.

[34] Z. Wang, X. Wang, and L. Liu, "Stochastic optimal linear control of wireless networked control systems with delays and packet losses," *IET Control Theory & Applications*, vol. 10, pp. 742-751, 2016.

[35] V. Kumar, K. P. S. Rana, and P. Mishra, "Robust speed control of hybrid electric vehicle using fractional order fuzzy PD and PI controllers in cascade control loop," *Journal of the Franklin Institute*, vol. 353, pp. 1713-1741, 2016.

[36] K. P. S. Rana, V. Kumar, N. Mittra, and N. Pramanik, "Implementation of fractional order integrator/differentiator on field programmable gate array," *Alexandria Engineering Journal*, vol. 55, pp. 1765-1773, 2016.

[37] A. Kumar and V. Kumar, "A novel interval type-2 fractional order fuzzy PID controller: design, performance evaluation, and its optimal time domain tuning," *ISA transactions*, vol. 68, pp. 251-275, 2017.

[38] M. Gheisarnejad and M. H. Khooban, "Design an optimal fuzzy fractional proportional integral derivative controller with derivative filter for load frequency control in power systems," *Transactions of the Institute of Measurement and Control*, p. 0142331218804309, 2019. DOI: 10.1177/0142331218804309

[39] M. El-Bardini and A. M. El-Nagar, "Interval type-2 fuzzy PID controller for uncertain nonlinear inverted pendulum system," *ISA transactions*, vol. 53, pp. 732-743, 2014.

[40] M. Gheisarnejad and M. H. Khooban, "Secondary load frequency control for multi-microgrids: HiL real-time simulation," *Soft Computing*, pp. 1-14, 2018. DOI: 10.1007/s00500-018-3243-5

[41] A. Hatamlou, "Black hole: A new heuristic optimization approach for data clustering," *Information sciences*, vol. 222, pp. 175-184, 2013.

[42] A. V. Chechkin, R. Metzler, J. Klafter, and V. Y. Gonchar, "Introduction to the theory of Lévy flights," *Anomalous transport: Foundations and applications*, vol. 49, pp. 431-451, 2008.

[43] M.-H. Khooban, "Secondary load frequency control of time-delay stand-alone microgrids with electric vehicles," *IEEE Transactions on Industrial Electronics*, vol. 65, pp. 7416-7422, 2018.

[44] H. Zhang, Y. Zhang, and C. Yin, "Hardware-in-the-loop simulation of robust mode transition control for a series–parallel hybrid electric vehicle," *IEEE Transactions on Vehicular Technology*, vol. 65, pp. 1059-1069, 2016.

[45] *https://www.nodc.noaa.gov/General/wave.html*.

[46] *www.solargis.info/doc/solar-and-pv-data [Online; accessed 10.10.14]*.